



# Oxidative dehydrogenation of *n*-butene to 1,3-butadiene over multicomponent bismuth molybdate ( $M^{II}_9Fe_3Bi_1Mo_{12}O_{51}$ ) catalysts: Effect of divalent metal ( $M^{II}$ )

Ji Chul Jung<sup>a</sup>, Howon Lee<sup>a</sup>, Jeong Gil Seo<sup>a</sup>, Sunyoung Park<sup>a</sup>, Young-Min Chung<sup>b</sup>, Tae Jin Kim<sup>b</sup>, Seong Jun Lee<sup>b</sup>, Seung-Hoon Oh<sup>b</sup>, Yong Seung Kim<sup>b</sup>, In Kyu Song<sup>a,\*</sup>

<sup>a</sup>School of Chemical and Biological Engineering, Institute of Chemical Processes, Seoul National University, Shinlim-dong, Kwanak-ku, Seoul 151-744, Republic of Korea

<sup>b</sup>SK Energy Corporation, Yuseong-ku, Daejeon 305-712, Republic of Korea

## ARTICLE INFO

### Article history:

Available online 31 July 2008

### Keywords:

Multicomponent bismuth molybdate  
Effect of divalent metal  
Oxidative dehydrogenation  
1,3-Butadiene  
Oxygen mobility

## ABSTRACT

Multicomponent bismuth molybdate ( $M^{II}_9Fe_3Bi_1Mo_{12}O_{51}$ ) catalysts with different divalent metal ( $M^{II}$  = Mg, Mn, Co, Ni, and Zn) were prepared by a co-precipitation method, and were applied to the oxidative dehydrogenation of *n*-butene to 1,3-butadiene. Effect of divalent metal ( $M^{II}$ ) on the catalytic performance of  $M^{II}_9Fe_3Bi_1Mo_{12}O_{51}$  catalysts was investigated. X-ray photoelectron spectroscopy (XPS) measurements were conducted to determine the oxygen mobility of  $M^{II}_9Fe_3Bi_1Mo_{12}O_{51}$  catalysts. It was found that the catalytic performance of  $M^{II}_9Fe_3Bi_1Mo_{12}O_{51}$  catalysts was closely related to the oxygen mobility of the catalysts. The yield for 1,3-butadiene was monotonically increased with increasing oxygen mobility of the catalysts. Among the catalysts tested, the  $Co_9Fe_3Bi_1Mo_{12}O_{51}$  catalyst with the highest oxygen mobility showed the best catalytic performance in the oxidative dehydrogenation of *n*-butene.

© 2008 Elsevier B.V. All rights reserved.

## 1. Introduction

Oxidative dehydrogenation of *n*-butene has been recognized as a promising process for producing 1,3-butadiene, an important raw material for manufacturing a large number of chemical products [1–4]. A number of catalysts have been investigated for the oxidative dehydrogenation of *n*-butene, including ferrite-type catalyst [5,6], Cu–Mo catalyst [7], vanadium-containing catalyst [8], and Bi–Mo-based catalyst [9–11]. Among these catalysts, Bi–Mo-based catalysts such as pure bismuth molybdates ( $\alpha$ - $Bi_2Mo_3O_{12}$ ,  $\beta$ - $Bi_2Mo_2O_9$ , and  $\gamma$ - $Bi_2MoO_6$ ) and multicomponent bismuth molybdates have been extensively studied as efficient catalysts for this reaction [12–15]. In particular, multicomponent bismuth molybdate catalysts have been widely investigated to improve the low-catalytic performance of pure bismuth molybdate catalysts [16–19]. However, only a few studies on the multicomponent bismuth molybdate catalysts have been reported in the literature [17–20], due to the difficulty in understanding their complicated compositions and structures. The reproducibility of the catalyst preparation is also one of the major issues to be solved in the multicomponent bismuth molybdate catalyst system. Therefore, developing an efficient multicomponent

bismuth molybdate catalyst for the oxidative dehydrogenation of *n*-butene would be a challenging work.

It is known that multicomponent bismuth molybdate catalysts have a general form of  $M^{II}_aM^{III}_bBi_cMo_dO_e$ , which includes divalent metal ( $M^{II}$ ), trivalent metal ( $M^{III}$ ), bismuth, and molybdenum [20–22]. Although a number of multicomponent bismuth molybdate catalysts can be formed depending on the constituent metal components and their compositions, it is generally accepted that Fe is the most suitable for  $M^{III}$  in the multicomponent bismuth molybdate catalyst system [16,22]. In our preliminary work investigating the effect of Fe content on the catalytic performance of  $Fe_xBi_1Mo_{12}O_{37.5+1.5x}$  ( $x = 1–4$ ) in the oxidative dehydrogenation of *n*-butene, it was found that the catalytic performance showed a volcano-shaped curve with respect to Fe content. Among the catalysts tested,  $Fe_3Bi_1Mo_{12}O_{42}$  showed the best catalytic performance, although fundamental reason for this has not been clearly understood yet. In our successive work [23], it was also revealed that the catalytic performance of  $Ni_xFe_3Bi_1Mo_{12}O_{42+x}$  ( $x = 2–10$ ) showed a volcano-shaped curve with respect to nickel content, and  $Ni_9Fe_3Bi_1Mo_{12}O_{51}$  exhibited the best catalytic performance in the reaction. Therefore,  $M^{II}_9Fe_3Bi_1Mo_{12}O_{51}$  was chosen as a model catalyst to investigate the effect of divalent metal on the catalytic performance of multicomponent bismuth molybdate in the oxidative dehydrogenation of *n*-butene.

Many researchers agree that the oxidative dehydrogenation of *n*-butene to 1,3-butadiene over multicomponent bismuth molyb-

\* Corresponding author. Tel.: +82 2 880 9227; fax: +82 2 889 7415.

E-mail address: [inksong@snu.ac.kr](mailto:inksong@snu.ac.kr) (I.K. Song).

date catalysts follows the Mars-van Krevelen mechanism [24,25]. According to this mechanism, oxygen in the multicomponent bismuth molybdate catalyst directly reacts with *n*-butene, and in turn, oxygen in the gas phase makes up oxygen vacancy in the catalyst. This means that oxygen mobility of the multicomponent bismuth molybdate catalyst plays a key role in determining the catalytic performance in the oxidative dehydrogenation of *n*-butene. Therefore, it is expected that a catalyst with high-oxygen mobility will show an excellent catalytic performance in the oxidative dehydrogenation of *n*-butene.

It has been reported that there are various oxygen species such as  $O_2^-$ ,  $O_2^{2-}$ ,  $O^-$ , and  $O^{2-}$  in the metal oxide catalyst [26,27]. Some researchers proposed that nucleophilic oxygen species such as  $O^{2-}$  were responsible for the selective oxidation of hydrocarbon, while electrophilic oxygen species such as  $O_2^-$ ,  $O_2^{2-}$ , and  $O^-$  were active for the total oxidation of hydrocarbon [27]. Although many attempts have been made to clarify the active oxygen species in the oxidation of hydrocarbon over metal oxide catalyst [28,29], this issue is still controversial. Therefore, this work was focused on not clarifying the active oxygen species for the reaction but determining the oxygen mobility of the catalyst involved in the reaction.

In this work, a series of multicomponent bismuth molybdate ( $M^{II}_9Fe_3Bi_1Mo_{12}O_{51}$ ) catalysts with different divalent metal ( $M^{II} = Mg, Mn, Co, Ni, \text{ and } Zn$ ) were prepared by a co-precipitation method, and were applied to the oxidative dehydrogenation of *n*-butene to 1,3-butadiene. The effect of divalent metal on the catalytic performance of  $M^{II}_9Fe_3Bi_1Mo_{12}O_{51}$  catalysts was investigated. X-ray photoelectron spectroscopy (XPS) measurements were conducted to determine the oxygen mobility of  $M^{II}_9Fe_3Bi_1Mo_{12}O_{51}$  catalysts, with an aim of elucidating their catalytic performance. A correlation between catalytic performance and oxygen mobility of  $M^{II}_9Fe_3Bi_1Mo_{12}O_{51}$  catalysts was then established.

## 2. Experimental

### 2.1. Preparation of $M^{II}_9Fe_3Bi_1Mo_{12}O_{51}$ catalysts

A wide set of  $M^{II}_9Fe_3Bi_1Mo_{12}O_{51}$  catalysts with different divalent metal ( $M^{II} = Mg, Mn, Co, Ni, \text{ and } Zn$ ) were prepared by a co-precipitation method at pH 1.0. Bismuth nitrate ( $Bi(NO_3)_3 \cdot 5H_2O$ , Sigma–Aldrich) (1.5 g) was dissolved in 10 ml of distilled water that had been acidified with 3 ml of concentrated nitric acid. The solution was then added to 100 ml of an aqueous solution containing known amount of divalent metal nitrate and 3.7 g of ferric nitrate ( $Fe(NO_3)_3 \cdot 9H_2O$ , Sigma–Aldrich) to obtain a mixed nitrate solution. Seven grams of magnesium nitrate ( $Mg(NO_3)_2 \cdot 6H_2O$ , Sigma–Aldrich), 7.8 g of manganese nitrate ( $Mn(NO_3)_2 \cdot 6H_2O$ , Sigma–Aldrich), 7.9 g of cobalt nitrate ( $Co(NO_3)_2 \cdot 6H_2O$ , Sigma–Aldrich), 7.9 g of nickel nitrate ( $Ni(NO_3)_2 \cdot 6H_2O$ , Sigma–Aldrich), and 8.1 g of zinc nitrate ( $Zn(NO_3)_2 \cdot 6H_2O$ , Sigma–Aldrich) were used as a divalent metal precursor for the preparation of  $M^{II}_9Fe_3Bi_1Mo_{12}O_{51}$  ( $M^{II} = Mg, Mn, Co, Ni, \text{ and } Zn$ ) catalysts. The mixed nitrate solution was added dropwise into 50 ml of an aqueous solution containing 6.4 g of ammonium molybdate ( $(NH_4)_6Mo_7O_{24} \cdot 4H_2O$ , Sigma–Aldrich) under vigorous stirring. After stirring the mixed solution vigorously at room temperature for 1 h, a solid product was obtained by evaporation. The solid product was dried overnight at 175 °C, and then it was calcined at 475 °C for 5 h in an air stream to yield the  $M^{II}_9Fe_3Bi_1Mo_{12}O_{51}$  catalyst.

### 2.2. Characterization

Formation of  $M^{II}_9Fe_3Bi_1Mo_{12}O_{51}$  ( $M^{II} = Mg, Mn, Co, Ni, \text{ and } Zn$ ) catalysts was confirmed by XRD (MAC Science, M18XHF-SRA) measurements. Atomic ratios of the prepared catalysts were

determined by ICP-AES (Shimadzu, ICP-1000IV) analyses. Surface areas of the catalysts were measured using a BET apparatus (Micromeritics, ASAP 2010). XPS analyses (Thermo VG, Sigma Probe) were conducted to measure the binding energies of O 1s of the  $M^{II}_9Fe_3Bi_1Mo_{12}O_{51}$  ( $M^{II} = Mg, Mn, Co, Ni, \text{ and } Zn$ ) catalysts, with an aim of determining the oxygen mobility of the catalysts. Binding energies of O 1s were calibrated using C 1s peak (284.5 eV) as a reference.

### 2.3. Oxidative dehydrogenation of *n*-butene

Oxidative dehydrogenation of *n*-butene to 1,3-butadiene was carried out in a continuous flow fixed-bed reactor in the presence of air and steam. Each catalyst (0.5 g) was pretreated at 470 °C for 1 h with an air stream (16 ml/min). Water was sufficiently vaporized by passing through a pre-heating zone and was continuously fed into the reactor together with *n*-butene and air. Based on our previous work [23], feed composition was fixed at *n*-butene: $O_2$ :steam = 1:0.75:15. *C*<sub>4</sub> raffinate-3 containing 57.9 wt% *n*-butene (1-butene (7.5 wt%) + *trans*-2-butene (33.9 wt%) + *cis*-2-butene (16.5 wt%)) was used as a *n*-butene source, and air was used as an oxygen source (nitrogen in air served as a carrier gas). *C*<sub>4</sub> raffinate-3 was composed of 57.9 wt% *n*-butene, 41.6 wt% *n*-butane, 0.3 wt% cyclobutane, 0.1 wt% methyl cyclopropane, and 0.1 wt% residue. The catalytic reaction was carried out at 420 °C. Gas hourly space velocity (GHSV) was fixed at 475 h<sup>−1</sup> on the basis of *n*-butene (the densities of  $M^{II}_9Fe_3Bi_1Mo_{12}O_{51}$  catalysts were almost the same). Reaction products were periodically sampled and analyzed with gas chromatographs. Conversion of *n*-butene and selectivity for 1,3-butadiene were calculated on the basis of carbon balance as follows. Yield for 1,3-butadiene was calculated by multiplying conversion and selectivity.

$$\text{Conversion of } n\text{-butene} = \frac{\text{moles of } n\text{-butene reacted}}{\text{moles of } n\text{-butene supplied}}$$

$$\text{Selectivity for 1, 3-butadiene} = \frac{\text{moles of 1, 3-butadiene formed}}{\text{moles of } n\text{-butene reacted}}$$

## 3. Results and discussion

### 3.1. Formation and characterization of $M^{II}_9Fe_3Bi_1Mo_{12}O_{51}$ catalysts

Successful formation of multicomponent bismuth molybdate ( $M^{II}_9Fe_3Bi_1Mo_{12}O_{51}$ ) catalysts was confirmed by XRD measurements. Fig. 1 shows the XRD patterns of  $M^{II}_9Fe_3Bi_1Mo_{12}O_{51}$  ( $M^{II} = Mg, Mn, Co, Ni, \text{ and } Zn$ ) catalysts. Each phase was identified by its characteristic diffraction peaks using JCPDS. It was found that  $M^{II}_9Fe_3Bi_1Mo_{12}O_{51}$  catalysts are composed of mixed phases of divalent metal molybdate ( $\alpha$ - $M^{II}MoO_4$  and/or  $\beta$ - $M^{II}MoO_4$ ),  $Fe_2(MoO_4)_3$ ,  $\alpha$ - $Bi_2Mo_3O_{12}$ , and  $\gamma$ - $Bi_2MoO_6$ . This result was well consistent with a previous report [16], indicating successful formation of  $M^{II}_9Fe_3Bi_1Mo_{12}O_{51}$  catalysts.

It is known that bismuth molybdates are located on the surface of the catalyst and serve as active phases, while divalent and trivalent metal molybdates are concentrated in the bulk of the catalyst and act as supports for the active components in the multicomponent bismuth molybdate catalyst system [16]. It has also been reported that metal molybdates (divalent and trivalent metal molybdates) in the bulk of the catalyst facilitate the migration of active oxygen species to the bismuth molybdates on the catalyst surface, leading to an enhanced oxygen mobility of multicomponent bismuth molybdate catalysts [18].

Fig. 1 clearly shows that the formation of divalent metal molybdate ( $M^{II}MoO_4$ ) in the  $M^{II}_9Fe_3Bi_1Mo_{12}O_{51}$  catalysts was

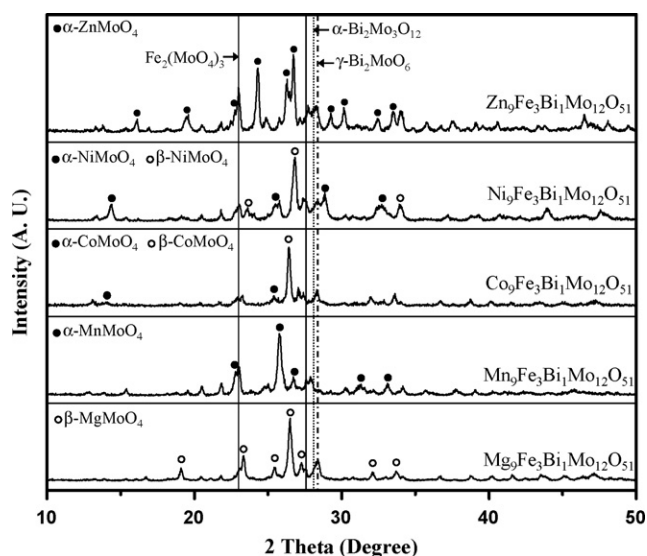


Fig. 1. XRD patterns of  $M^{\text{II}}_9\text{Fe}_3\text{Bi}_1\text{Mo}_{12}\text{O}_{51}$  ( $M^{\text{II}} = \text{Mg, Mn, Co, Ni, and Zn}$ ) catalysts.

different depending on the identity of divalent metal species ( $M^{\text{II}}$ ). This indicates that  $M^{\text{II}}_9\text{Fe}_3\text{Bi}_1\text{Mo}_{12}\text{O}_{51}$  catalysts with different divalent metal may retain different ability for migrating active oxygen species to the bismuth molybdates on the catalyst surface. When taking into account of the fact that oxygen mobility of the catalyst plays a key role in determining the catalytic performance in the oxidative dehydrogenation of *n*-butene, it is reasonable to expect that  $M^{\text{II}}_9\text{Fe}_3\text{Bi}_1\text{Mo}_{12}\text{O}_{51}$  catalysts with different divalent metal would show a different catalytic performance in the oxidative dehydrogenation of *n*-butene.

Atomic ratios of constituent metal components are summarized in Table 1. The atomic ratio of a metal component was calculated as the ratio of the amount of each metal component ( $M^{\text{II}}$ , Fe, and Mo) with respect to that of Bi. The atomic ratios determined by ICP-AES analyses are in good agreement with the theoretical values, indicating successful formation of  $M^{\text{II}}_9\text{Fe}_3\text{Bi}_1\text{Mo}_{12}\text{O}_{51}$  catalysts. BET surface areas of  $M^{\text{II}}_9\text{Fe}_3\text{Bi}_1\text{Mo}_{12}\text{O}_{51}$  catalysts are also summarized in Table 1. The BET surface areas were in the range of 2.2–17.5  $\text{m}^2/\text{g}$ . However, no reliable correlation between BET surface area (Table 1) and catalytic performance (Fig. 2) of  $M^{\text{II}}_9\text{Fe}_3\text{Bi}_1\text{Mo}_{12}\text{O}_{51}$  catalysts was observed (although it is not shown here).

### 3.2. Catalytic performance of $M^{\text{II}}_9\text{Fe}_3\text{Bi}_1\text{Mo}_{12}\text{O}_{51}$ catalysts

Fig. 2 shows the steady-state catalytic performance of  $M^{\text{II}}_9\text{Fe}_3\text{Bi}_1\text{Mo}_{12}\text{O}_{51}$  ( $M^{\text{II}} = \text{Mg, Mn, Co, Ni, and Zn}$ ) catalysts in the oxidative dehydrogenation of *n*-butene at 420 °C after a 6-h reaction. Although the catalytic performance with time on stream

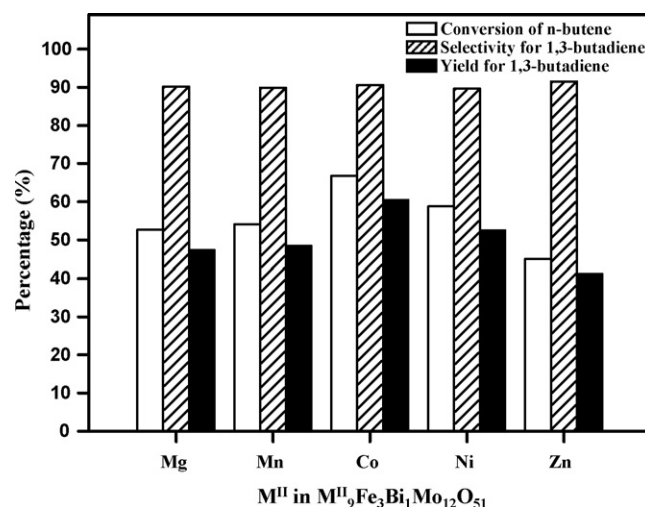


Fig. 2. Steady-state catalytic performance of  $M^{\text{II}}_9\text{Fe}_3\text{Bi}_1\text{Mo}_{12}\text{O}_{51}$  ( $M^{\text{II}} = \text{Mg, Mn, Co, Ni, and Zn}$ ) catalysts in the oxidative dehydrogenation of *n*-butene at 420 °C after a 6-h reaction.

was not shown here, all the  $M^{\text{II}}_9\text{Fe}_3\text{Bi}_1\text{Mo}_{12}\text{O}_{51}$  catalysts showed a steady-state catalytic performance after a 3-h reaction. In our catalytic reaction,  $\text{CO}_2$  was mainly produced as a by-product and CO formation was negligible. Selectivity for 1,3-butadiene was almost constant (ca. 90%). However, conversion of *n*-butene was different depending on the identity of divalent metal species. Consequently, yield for 1,3-butadiene, which was calculated by multiplying conversion and selectivity, showed the same trend as conversion of *n*-butene. Among the catalysts tested, the  $\text{Co}_9\text{Fe}_3\text{Bi}_1\text{Mo}_{12}\text{O}_{51}$  catalyst showed the best catalytic performance in terms of conversion of *n*-butene and yield for 1,3-butadiene, indicating that Co was the most suitable divalent metal component ( $M^{\text{II}}$ ) for the multicomponent bismuth molybdate ( $M^{\text{II}}_9\text{Fe}_3\text{Bi}_1\text{Mo}_{12}\text{O}_{51}$ ) catalyst system.

$\text{Co}_x\text{Ni}_{9-x}\text{Fe}_3\text{Bi}_1\text{Mo}_{12}\text{O}_{51}$  ( $x = 1-8$ ) catalysts were also prepared with an aim of investigating any synergistic effect of two divalent metal components in the reaction. However,  $\text{Co}_x\text{Ni}_{9-x}\text{Fe}_3\text{Bi}_1\text{Mo}_{12}\text{O}_{51}$  ( $x = 1-8$ ) catalysts did not show a higher catalytic performance than  $\text{Co}_9\text{Fe}_3\text{Bi}_1\text{Mo}_{12}\text{O}_{51}$  in the reaction, indicating that any combinations of two divalent metal components were not efficient for the oxidative dehydrogenation of *n*-butene.

### 3.3. Oxygen mobility of $M^{\text{II}}_9\text{Fe}_3\text{Bi}_1\text{Mo}_{12}\text{O}_{51}$ catalysts

Oxygen mobility of various metal oxide catalysts has been measured using various experimental tools such as  $^{18}\text{O}/^{16}\text{O}$  isotope exchange [29,30], TPR (temperature-programmed reduction) [29], TPRO (temperature-programmed reoxidation) [31],  $\text{O}_2$ -TPD (temperature-programmed desorption) [26,29], and XPS measurements [27]. Among these experimental techniques, XPS has served as a powerful tool for measuring oxygen mobility of the catalyst. In this work, we also measured the binding energies of O 1s of  $M^{\text{II}}_9\text{Fe}_3\text{Bi}_1\text{Mo}_{12}\text{O}_{51}$  catalysts in order to determine the oxygen mobility of the catalysts.

In the multicomponent bismuth molybdate catalyst, it was reported that bulk oxygen in the catalyst provided the active oxygen species for the reaction through the migration to the surface on the catalyst [16]. However, the catalytic performance of multicomponent bismuth molybdate is not related to the bulk oxygen mobility of the catalyst but related to the surface oxygen mobility of the catalyst, because the surface oxygen of the catalyst directly takes part in the reaction. In this work, therefore, only the

Table 1

Atomic ratios and BET surface areas of  $M^{\text{II}}_9\text{Fe}_3\text{Bi}_1\text{Mo}_{12}\text{O}_{51}$  ( $M^{\text{II}} = \text{Mg, Mn, Co, Ni, and Zn}$ ) catalysts

Catalyst	Atomic ratio				BET surface area ( $\text{m}^2/\text{g}$ )
	$M^{\text{II}}$	Fe	Bi	Mo	
$\text{Mg}_9\text{Fe}_3\text{Bi}_1\text{Mo}_{12}\text{O}_{51}$	8.7 (Mg)	3.0	1.0	11.5	3.1
$\text{Mn}_9\text{Fe}_3\text{Bi}_1\text{Mo}_{12}\text{O}_{51}$	9.1 (Mn)	3.1	1.0	11.3	12.3
$\text{Co}_9\text{Fe}_3\text{Bi}_1\text{Mo}_{12}\text{O}_{51}$	9.0 (Co)	3.2	1.0	11.4	2.3
$\text{Ni}_9\text{Fe}_3\text{Bi}_1\text{Mo}_{12}\text{O}_{51}$	8.7 (Ni)	3.2	1.0	12.0	17.5
$\text{Zn}_9\text{Fe}_3\text{Bi}_1\text{Mo}_{12}\text{O}_{51}$	8.6 (Zn)	3.1	1.0	12.0	2.2

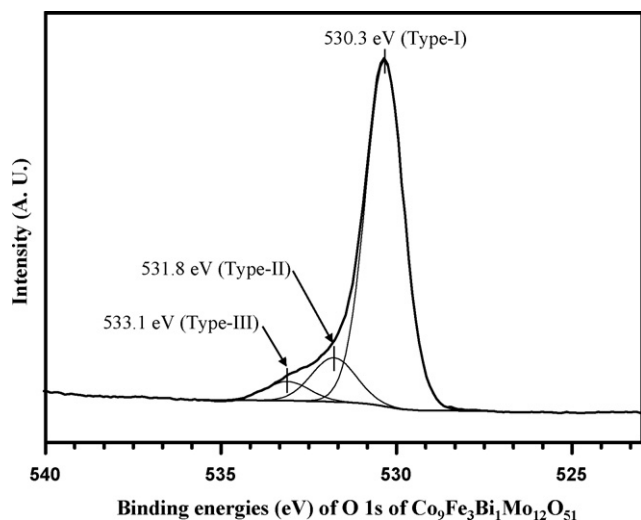


Fig. 3. XPS spectrum of O 1s of  $\text{Co}_9\text{Fe}_3\text{Bi}_1\text{Mo}_{12}\text{O}_{51}$  catalyst.

surface oxygen mobility of the catalysts was determined by XPS measurements.

Fig. 3 shows the XPS spectrum of O 1s of  $\text{Co}_9\text{Fe}_3\text{Bi}_1\text{Mo}_{12}\text{O}_{51}$  catalyst. Deconvolution of O 1s spectrum reveals that there are three types of surface oxygen species in the  $\text{Co}_9\text{Fe}_3\text{Bi}_1\text{Mo}_{12}\text{O}_{51}$  catalyst (denoted as Type-I, -II, and -III in the order of increasing binding energy). These three types of oxygen species were also observed in all the  $\text{M}^{\text{II}}_9\text{Fe}_3\text{Bi}_1\text{Mo}_{12}\text{O}_{51}$  catalysts. The binding energies of O 1s of  $\text{M}^{\text{II}}_9\text{Fe}_3\text{Bi}_1\text{Mo}_{12}\text{O}_{51}$  ( $\text{M}^{\text{II}}$  = Mg, Mn, Co, Ni, and Zn) catalysts are summarized in Table 2. It is interesting to note that binding energies of Type-I oxygen species are almost identical, while those of Type-II and -III oxygen species are different depending on the identity of divalent metal of the  $\text{M}^{\text{II}}_9\text{Fe}_3\text{Bi}_1\text{Mo}_{12}\text{O}_{51}$  catalysts.

It is believed that Type-III oxygen with the highest binding energy (532.5–533.1 eV) corresponds to the oxygen species weakly bonded on the catalyst surface. This means that Type-III oxygen is not the oxygen species responsible for the oxidative dehydrogenation of *n*-butene. In fact, the binding energy of Type-III oxygen was not directly correlated with the catalytic performance of  $\text{M}^{\text{II}}_9\text{Fe}_3\text{Bi}_1\text{Mo}_{12}\text{O}_{51}$  catalysts (this is not shown here). In our previous work measuring the oxygen mobility of  $\text{Ni}_9\text{Fe}_3\text{Bi}_1\text{Mo}_{12}\text{O}_{51}$  catalysts prepared at different pH [32], it was revealed that the binding energy of Type-II oxygen reflected the oxygen mobility of the multicomponent bismuth molybdate catalysts. In this work, therefore, the binding energy of Type-II oxygen was used as an index for the oxygen mobility of the catalyst.

It is expected that the binding energy of O 1s of the metal oxide catalyst is different depending on the strength of metal–oxygen bond in the catalyst. The binding energy of O 1s of the metal oxide catalyst increases with decreasing valence electron density of lattice oxygen. The decrement of valence electron density of lattice

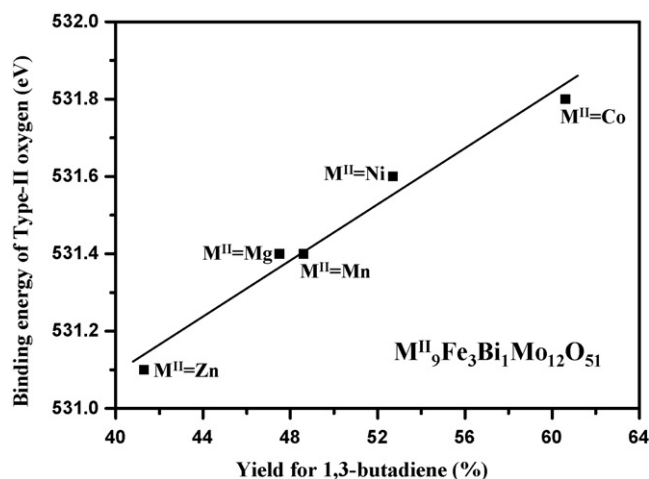


Fig. 4. A correlation between yield for 1,3-butadiene and binding energy of Type-II oxygen of  $\text{M}^{\text{II}}_9\text{Fe}_3\text{Bi}_1\text{Mo}_{12}\text{O}_{51}$  ( $\text{M}^{\text{II}}$  = Mg, Mn, Co, Ni, and Zn) catalysts.

oxygen implies the decrement of coulombic force between metal cation and oxygen anion. It is believed that the lattice oxygen weakly bonded to metal cation is more mobile and active. Therefore, it can be inferred that metal–oxygen bond in the catalyst would be weakened with increasing binding energy of O 1s, making the lattice oxygen more active and mobile [27]. In other words, the higher binding energy of O 1s corresponds to the higher oxygen mobility.

Undoubtedly, it is unfavorable if oxygen species responsible for the total oxidation of *n*-butene are more mobile and active. As mentioned above, however, Type-II oxygen is not the oxygen species involved in the total oxidation of *n*-butene but the oxygen species responsible for the oxidative dehydrogenation of *n*-butene. Therefore, an investigation on the oxygen mobility of the catalyst using XPS measurements was focused on the Type-II oxygen.

#### 3.4. Correlation between catalytic performance and oxygen mobility of $\text{M}^{\text{II}}_9\text{Fe}_3\text{Bi}_1\text{Mo}_{12}\text{O}_{51}$

Fig. 4 shows a comprehensive correlation between yield for 1,3-butadiene and binding energy of Type-II oxygen of  $\text{M}^{\text{II}}_9\text{Fe}_3\text{Bi}_1\text{Mo}_{12}\text{O}_{51}$  ( $\text{M}^{\text{II}}$  = Mg, Mn, Co, Ni, and Zn) catalysts. Catalytic performance data were taken from Fig. 2. The correlation clearly shows that the catalytic performance of  $\text{M}^{\text{II}}_9\text{Fe}_3\text{Bi}_1\text{Mo}_{12}\text{O}_{51}$  catalysts is closely related to the oxygen mobility of the catalysts. The yield for 1,3-butadiene was monotonically increased with increasing binding energy of Type-II oxygen, that is, with increasing oxygen mobility of the catalyst. Among the catalysts tested, the  $\text{Co}_9\text{Fe}_3\text{Bi}_1\text{Mo}_{12}\text{O}_{51}$  catalyst with the highest binding energy of Type-II oxygen showed the best catalytic performance in the oxidative dehydrogenation of *n*-butene. It can be concluded that oxygen mobility is one of the crucial factors determining the catalytic performance of  $\text{M}^{\text{II}}_9\text{Fe}_3\text{Bi}_1\text{Mo}_{12}\text{O}_{51}$  catalysts in the oxidative dehydrogenation of *n*-butene.

#### 4. Conclusions

Multicomponent bismuth molybdate ( $\text{M}^{\text{II}}_9\text{Fe}_3\text{Bi}_1\text{Mo}_{12}\text{O}_{51}$ ) catalysts with different divalent metal ( $\text{M}^{\text{II}}$  = Mg, Mn, Co, Ni, and Zn) were prepared by a co-precipitation method, and were applied to the oxidative dehydrogenation of *n*-butene to 1,3-butadiene. Successful formation of  $\text{M}^{\text{II}}_9\text{Fe}_3\text{Bi}_1\text{Mo}_{12}\text{O}_{51}$  catalysts was well confirmed by XRD and ICP-AES analyses. XPS measurements were conducted to determine the oxygen mobility of  $\text{M}^{\text{II}}_9\text{Fe}_3\text{Bi}_1\text{Mo}_{12}\text{O}_{51}$

Table 2  
Binding energies of O 1s of  $\text{M}^{\text{II}}_9\text{Fe}_3\text{Bi}_1\text{Mo}_{12}\text{O}_{51}$  ( $\text{M}^{\text{II}}$  = Mg, Mn, Co, Ni, and Zn) catalysts

Catalyst	Binding energy (eV) of O 1s		
	Type-I	Type-II	Type-III
$\text{Mg}_9\text{Fe}_3\text{Bi}_1\text{Mo}_{12}\text{O}_{51}$	530.2	531.4	532.6
$\text{Mn}_9\text{Fe}_3\text{Bi}_1\text{Mo}_{12}\text{O}_{51}$	530.3	531.4	532.6
$\text{Co}_9\text{Fe}_3\text{Bi}_1\text{Mo}_{12}\text{O}_{51}$	530.3	531.8	533.1
$\text{Ni}_9\text{Fe}_3\text{Bi}_1\text{Mo}_{12}\text{O}_{51}$	530.2	531.6	533.1
$\text{Zn}_9\text{Fe}_3\text{Bi}_1\text{Mo}_{12}\text{O}_{51}$	530.2	531.1	532.5

catalysts. It was revealed that the catalytic performance of  $M^{II}_9Fe_3Bi_1Mo_{12}O_{51}$  was well correlated with the oxygen mobility of the catalysts. The yield for 1,3-butadiene was monotonically increased with increasing oxygen mobility of  $M^{II}_9Fe_3Bi_1Mo_{12}O_{51}$  catalysts. Oxygen mobility played an important role in determining the catalytic performance of  $M^{II}_9Fe_3Bi_1Mo_{12}O_{51}$  catalysts in the oxidative dehydrogenation of *n*-butene. Among the catalysts tested, the  $Co_9Fe_3Bi_1Mo_{12}O_{51}$  catalyst showed the best catalytic performance. It is expected that a more efficient catalyst than  $Co_9Fe_3Bi_1Mo_{12}O_{51}$  catalyst for the oxidative dehydrogenation of *n*-butene can be developed by the suitable modification of  $Co_9Fe_3Bi_1Mo_{12}O_{51}$  catalyst.

## Acknowledgement

The authors wish to acknowledge support from the Korea Energy Management Corporation (2005-01-0090-3-010).

## References

- [1] S.C. Oh, H.P. Lee, H.T. Kim, K.O. Yoo, Kor. J. Chem. Eng. 16 (1999) 543.
- [2] Ph.A. Batist, J.F.H. Bouwens, G.C.A. Schuit, J. Catal. 25 (1972) 1.
- [3] R.K. Grasselli, Top. Catal. 21 (2002) 79.
- [4] W.J. Linn, A.W. Sleight, J. Catal. 41 (1976) 134.
- [5] H. Lee, J.C. Jung, H. Kim, Y.-M. Chung, T.J. Kim, S.J. Lee, S.-H. Oh, Y.S. Kim, I.K. Song, Catal. Commun. 9 (2008) 1137.
- [6] J.M. López Nieto, P. Concepción, A. Dejoz, H. Knözinger, F. Melo, M.I. Vázquez, J. Catal. 189 (2000) 147.
- [7] P.N. Tiwari, T.G. Alkhozov, K.U. Adzhamov, A.K. Khanmamedova, J. Catal. 120 (1989) 278.
- [8] J.A. Toledo-Antonio, N. Nava, M. Matínez, X. Bokhimi, Appl. Catal. A 234 (2002) 137.
- [9] D.A.G. van Oeffelen, J.H.C. van Hooff, G.C.A. Schuit, J. Catal. 95 (1985) 84.
- [10] M. Egashira, K. Matsuo, S. Kagawa, T. Seiyama, J. Catal. 58 (1979) 409.
- [11] Ph.A. Batist, B.C. Lippens, G.C.A. Schuit, J. Catal. 5 (1966) 55.
- [12] L.M. Madeira, M.F. Portela, Catal. Rev. 44 (2002) 247.
- [13] A.P.V. Soares, L.D. Dimitrov, M.C.A. Oliveira, L. Hilaire, M.F. Portela, R.K. Grasselli, Appl. Catal. A 253 (2003) 191.
- [14] J.C. Jung, H. Kim, A.S. Choi, Y.-M. Chung, T.J. Kim, S.J. Lee, S.-H. Oh, I.K. Song, J. Mol. Catal. A 259 (2006) 166.
- [15] E.V. Hoefs, J.R. Monnier, G.W. Keulks, J. Catal. 57 (1979) 331.
- [16] Y. Moro-oka, W. Ueda, Adv. Catal. 40 (1994) 233.
- [17] M.W.J. Wolfs, Ph.A. Batist, J. Catal. 32 (1974) 25.
- [18] D.-H. He, W. Ueda, Y. Moro-oka, Catal. Lett. 12 (1992) 35.
- [19] W. Ueda, K. Asakawa, C.-L. Chen, Y. Moro-oka, T. Ikawa, J. Catal. 101 (1986) 360.
- [20] C.F. Cullis, D.J. Hucknall, in: G.C. Bond, G. Webb (Eds.), A Specialist Periodical Report: Catalysis, vol. 5, Royal Chemical Society, London, 1982, p. 273.
- [21] R.K. Grasselli, J.D. Burrington, Adv. Catal. 30 (1981) 133.
- [22] H.H. Kung, M.C. Kung, Adv. Catal. 33 (1985) 159.
- [23] J.C. Jung, H. Lee, H. Kim, Y.-M. Chung, T.J. Kim, S.J. Lee, S.-H. Oh, Y.S. Kim, I.K. Song, Catal. Commun. 9 (2008) 447.
- [24] M.F. Portela, Top. Catal. 15 (2001) 241.
- [25] R.K. Grasselli, in: G. Ertl, H. Knözinger, J. Weitkamp (Eds.), Handbook of Heterogeneous Catalysis, vol. 5, Wiley, New York, 1997, p. 2302.
- [26] S. Royer, D. Duprez, S. Kaliaguine, Catal. Today 112 (2006) 99.
- [27] H.X. Dai, C.F. Ng, C.T. Au, J. Catal. 189 (2000) 52.
- [28] X. Zhang, Y. Gong, G. Yu, Y. Xie, J. Mol. Catal. A 180 (2002) 293.
- [29] H. He, H.X. Dai, C.T. Au, Catal. Today 90 (2004) 245.
- [30] H. He, H.X. Dai, K.W. Wong, C.T. Au, Appl. Catal. A 251 (2003) 61.
- [31] S. Sugiyama, T. Hashimoto, Y. Tanabe, N. Shigemoto, H. Hayashi, J. Mol. Catal. A 227 (2005) 255.
- [32] J.C. Jung, H. Lee, H. Kim, Y.-M. Chung, T.J. Kim, S.J. Lee, S.-H. Oh, Y.S. Kim, I.K. Song, Catal. Commun. 9 (2008) 943.